

# Computational Fluid Dynamics (CFD) Simulations of Dispersed Flow of Viscous Oil in Water in a Horizontal Pipe

\*Robin Yap Miao Sin, Cary K Turangan

Institute of High Performance Computing, 1 Fusionopolis Way, #16-16 Connexis, Singapore

\*Corresponding author: yapmsr@ihpc.a-star.edu.sg

## Abstract

Heavy oil is a type of crude oil that has higher viscosity and heavier molecular composition than conventional oil, which make heavy oil very challenging to transport by means of pipelines. Our objective is to study and establish a methodology via Computational Fluid Dynamics (CFD) simulations on transportation of viscous oil in pipes in the form of dispersed oil droplets in water. Numerical simulations with *Eulerian-Eulerian* scheme are performed to model experimental tests of oil-in-water dispersed flow. In the simulations, two parameters (lift coefficient  $C_L$  and oil droplet diameter  $d$ ) are assumed to be constant. Oil superficial-velocity,  $J_o$ , is also kept constant at 0.64m/s, and water superficial-velocity,  $J_w$ , ranges from 2.20m/s to 2.60m/s. Simulation shows that positive  $C_L$  and large oil droplet diameters gives results resembling the experimental observation. In particular,  $C_L$  of 0.01 and oil drop diameter  $d$  of 4.0mm or 8.0mm show a good agreement with the experiment. The results show some valuable insights into the mechanisms of dispersed oil-in-water flow to provide further understanding on its flow mechanism.

**Keywords:** Viscous oil, dispersed oil-in-water, CFD simulations, pipe flow

## 1. Introduction

Heavy oil is a type of oil which is characterized by its heavier molecular composition and higher viscosity, which makes transportation difficult along pipeline. At present, it is estimated that heavy oil accounts for 70% of the global crude oil reserves (Alboudwarej *et al.*, 2006). As conventional crude oil reserve is scarce, heavy oil becomes more attractive alternative. The present research efforts associated with heavy crude oil have been on the extraction, transportation and production. In practice, the most common method of transporting heavy oil is via dispersed flow of oil in water. It has also been suggested that core-annular flow where the oil core is flowing at the core of the pipe and surrounded by a water layer flowing in the annulus can be another promising alternative (Bannwart *et al.*, 2012). Core-annular flow is considered a revolutionary method but still needs further development in terms of flow initiation and control. For dispersed flow, oil droplets are normally dispersed in water. Our main focus in the present work is to investigate the flow of viscous oil that represents heavy oil via dispersed flow along a horizontal pipe using numerical simulations.

There have been substantial experimental works on the two-phase flow of oil and water in horizontal and vertical pipelines including those on two-phase flow of low viscosity oil conducted by Lovick and Angeli (2004) and Hu and Angeli (2006). Lovick and Angeli (2004) studied the dual continuous flow pattern in oil-water flows in a 38.0mm-diameter, horizontal, stainless steel pipe using water and oil (oil viscosity  $\mu_o = 6\text{mPa}\cdot\text{s}$ , oil density  $\rho_o = 828\text{kg/m}^3$ ). Measurements were made for mixture velocities from 0.8m/s to 3.0m/s and input oil volume fractions from 0.1 to 0.9. They found that velocity ratio increased with increasing input oil fraction, and for high oil fractions it was above 1.0. At the highest mixture

velocities, it was reduced to values below 1.0. Hu and Angeli (2006) studied co-current upward and downward oil-water flows in a vertical stainless steel pipe of 38.0mm in diameter. Oil ( $\mu_o = 5.5\text{mPa}\cdot\text{s}$ ,  $\rho_o = 828\text{kg}/\text{m}^3$ ) and tap water were used as test fluids. The flow pattern changed from water-in-oil dispersion to oil-in-water dispersion. The mixture velocity was varied from 1.5m/s to 2.5m/s for upflow and downflow. Oil input-ratio was varied from 0 to 1.0. The in-situ oil hold-up and velocity ratio were investigated at different mixture velocity and input oil fraction.

Other works on two-phase flow of high viscosity oil and water were conducted by Charles *et al.* (1961), Bai *et al.* (1992), Bannwart *et al.* (2004), Sotgia *et al.* (2008) and Wang *et al.* (2011). Charles *et al.* (1961) investigated two-phase flow of high viscosity oil and water in a horizontal pipe of 26.4mm (1.04in) in diameter. Oil with viscosities of {0.00629, 0.0168, 0.065} Pa.s was used. Flow patterns, holdup ratios and pressure gradients were investigated for a range of superficial oil velocity,  $J_o$ , from 0.0152m/s to 0.914m/s and a range of superficial water velocity,  $J_w$ , from 0.0305m/s to 0.107m/s with input oil-water ratios ranging from 0.1 to 10.0.

Bai (1992) investigated the upflow and downflow of oil and water in a vertical pipe. Oil ( $\rho_o = 905\text{kg}/\text{m}^3$ ,  $\mu_o = 0.601\text{kg}/\text{ms}$ ) and water ( $\rho_w = 995\text{kg}/\text{m}^3$ ,  $\mu_w = 0.001\text{kg}/\text{ms}$ ) are used as test fluids. The flow pattern changes from oil bubbles in water to dispersions. Dimensionless pressure gradient as a function of input ratio for various values of water flow velocity from 0.101m/s to 0.853m/s were investigated. Bannwart *et al.* (2004) studied the flow patterns formed by heavy crude oil ( $\rho_o = 925.5\text{kg}/\text{m}^3$ ,  $\mu_o = 488\text{mPa}\cdot\text{s}$  at 20°C) inside vertical and horizontal pipe of 2.84cm in diameter. The annular flow pattern (“core annular flow”) was observed in both horizontal and vertical test sections at low water input fractions.

Sotgia *et al.* (2008) performed an experimental study of water continuous oil-water flow in horizontal pipes using mineral oil ( $\mu_o = 0.919\text{Pa}\cdot\text{s}$ ,  $\rho_o = 889\text{kg}/\text{m}^3$  at 20°C) and tap water ( $\mu_w = 1.026 \times 10^{-3}\text{Pa}\cdot\text{s}$ ). The oil-water interfacial tension is  $\sigma = 20 \times 10^{-3}\text{N}/\text{m}$ . A set of seven different pipes of Pyrex and Plexiglas with diameters ranging from 21.0 to 40.0 mm were used. Flow patterns for  $J_o = 0.50\text{m}/\text{s}$  and  $J_w = 0.11\text{m}/\text{s}$  to 2.51m/s were observed in the 26.0mm Plexiglas tube. In addition, flow patterns for  $J_o = 0.48\text{m}/\text{s}$  and  $J_w = 0.05\text{m}/\text{s}$  to 1.11m/s were observed in the 40.0mm Pyrex tube. Pressure drop reduction factor,  $R$  were measured in the 26.0mm Plexiglass for  $J_o = 0.21\text{m}/\text{s}$  to 0.97m/s at water input ratio,  $\varepsilon_w$ , from 0.1 to 0.9.

## 2. Computational domain and methodology

The computational domain of the simulations presented here is modelled after the experimental set-up by Sotgia *et al.* (2008). The length of the pipe,  $L$ , is 5.0m and inner diameter,  $\Phi$ , is 26.0mm. The geometry was meshed using polyhedral cells of approximately 470 thousand cells (Figure 1). The boundary condition for the inlet is *velocity inlet* and the outlet is *pressure outlet*. The water input ratio is  $\varepsilon_w = J_w / (J_w + J_o)$ , where  $J_w$  and  $J_o$  are water and oil superficial velocity, respectively. At outlet, the (gauge) pressure was set to 0. The actual velocity of the phase is  $V_p = J_p / \alpha_p$ , where  $J_p$  is the superficial velocity of the phase and  $\alpha_p$  volume fraction of the phase.

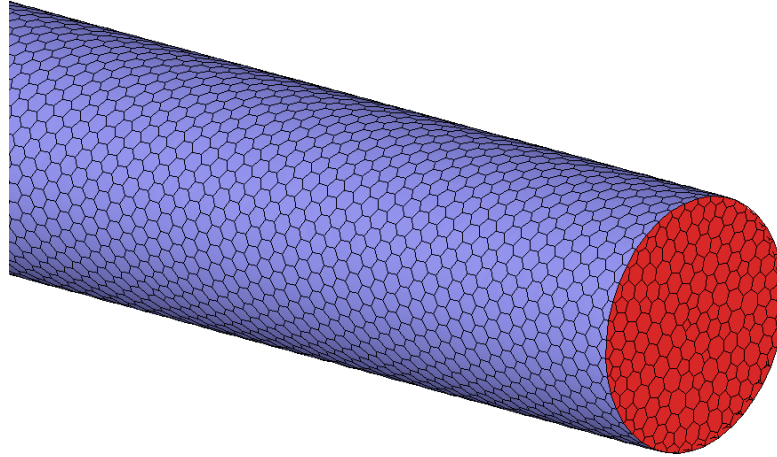


**Figure 1. A plot of the computational mesh on the surface of the pipe showing polyhedral cell types. The pipe was discretized using 470 thousand polyhedral cells. Pipe length  $L = 5.0$  m and diameter  $\Phi = 26.0$  mm.**

The flow physics inside the pipe was solved using computational fluid dynamics (CFD) solver ANSYS Fluent. The steady state simulations were performed, and gravitational force was taken into account. As the simulation involved interaction between two fluids, Eulerian multiphase model was implemented. For this model, water is assumed to be the continuous phase, and the oil is represented using droplets with finite diameters. It is also assumed that the droplets are spherical in shape throughout the simulations. Because for this particular flow conditions, the flow is turbulent,  $k-\varepsilon$  turbulence model of *Realizable* type was used.

Thermodynamic properties of oil and water follow those given by Sotgia *et al.* (2008). For oil, the density and viscosity are  $\rho_o = 889\text{kg/m}^3$  and  $\mu_o = 0.919\text{Pa.s}$ , respectively. For water, the density and viscosity are  $\rho_w = 998\text{kg/m}^3$  and  $\mu_w = 1.026 \times 10^{-3}\text{Pa.s}$ , respectively. The oil-water interfacial tension  $\sigma = 20 \times 10^{-3}\text{N/m}$ . The oil drops were assumed to be spherical in shape with constant diameter ranged from 1.0mm to 8.0 mm. The lift coefficient,  $C_L$ , on the oil drop ranged from -0.50 to 0.50. In addition, the drag coefficient,  $C_D$ , was also taken into account.

### 3. Results and Discussions

#### 3.1. Effects of lift coefficient, $C_L$

The effects of lift coefficient,  $C_L$ , on dispersed flow were investigated at oil superficial velocity  $J_o = 0.64\text{m/s}$  and water superficial velocity  $J_w = 2.20\text{m/s}$ . The oil drop diameter was kept constant at 1.0mm. Simulation was done for  $C_L = -0.50, 0, 0.10$  and 0.50. Figure 2 shows the phase contour of the cross section of the pipe at 4.5m from the inlet. At  $C_L = -0.50$ , water is at the core and oil is at the annulus of the pipe. At  $C_L = 0$ , oil appears to be scattered with a greater concentration of water ( $\alpha_w = 0.775$ ) at the core. At  $C_L = 0.10$ , oil appears to be scattered with a greater concentration of oil ( $\alpha_o = 0.23$ ) at the core. At  $C_L = 0.50$ , oil is at the core and water is at the annulus of the pipe. The results at  $C_L = 0.10$  and 0.50 are more consistent with the experiment as the phase contour shows dispersed flow with a greater concentration of oil at the core as compared with the annulus. From the results, we may deduce that the lift coefficient acting on the oil droplets may be between 0.10 and 0.50 for an oil drop diameter of 1.0mm.

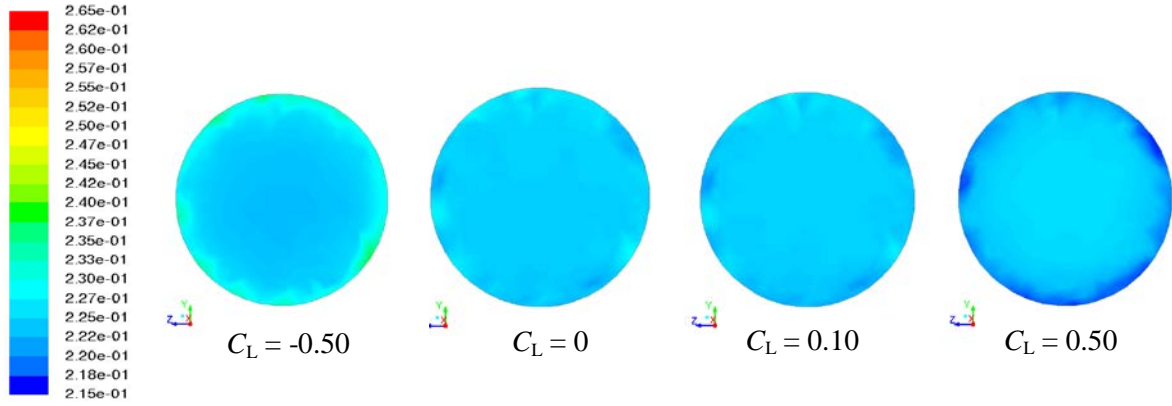


**Figure 2.** Plot of volume fraction of oil at different  $C_L$  for dispersed flow of oil drop diameter  $d = 1.0$  mm. Positive  $C_L$  resembles more closely with experiment as compared with negative  $C_L$ .

### 3.2. Effects of oil drop diameter, $d$

The effects of oil drop diameters,  $d$ , for different lift coefficient,  $C_L$ , on dispersed flow were further investigated. The oil drop diameter was kept constant and ranges from 1.0mm, 2.0mm, 4.0mm and 8.0mm. The effects of lift coefficient,  $C_L$  on dispersed flow were investigated at 0.01, 0.10 and 0.50. The plot of the phase contours from the simulation results are shown in Figure 3. At  $C_L = 0.01$  and  $d = 1.0$ mm or 2.0mm, the oil drop appears to be scattered ( $\alpha_o = 0.214$ ). At  $C_L = 0.01$  and  $d = 4.0$ mm, there is a higher concentration oil at the core ( $\alpha_o = 0.214$ ) as compared with the annulus ( $\alpha_o = 0.211$ ) and the core is displaced vertically upwards. The oil core was surrounded by a higher concentration of water. At  $C_L = 0.01$  and  $d = 8.0$ mm, oil appears to be concentric at the core ( $\alpha_o = 0.217$ ) which is displaced vertically upwards. The oil core was surrounded by an annulus having a lower concentration of oil ( $\alpha_o = 0.208$ ).

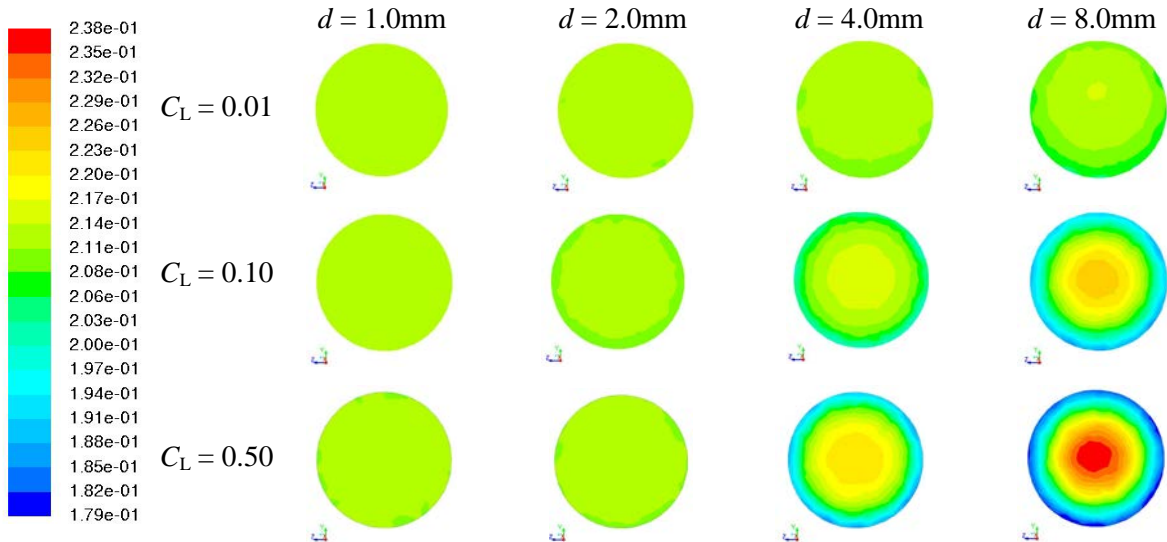


**Figure 3.** Plots of volume fraction of oil at different oil drop diameter,  $d$  and  $C_L$  for dispersed flow.  $C_L = 0.01$  and  $d = 4.0$ mm or 8.0mm resemble more closely with the experiment as oil core is displaced vertically upwards.

At  $C_L = 0.10$  and  $d = 1.0$ mm, oil appears to be scattered. At  $C_L = 0.10$  and  $d = 2.0$ mm, there is a higher concentration of oil at the core ( $\alpha_o = 0.214$ ) as compared with the annulus ( $\alpha_o =$

0.208). At  $C_L = 0.10$  and  $d = 4.0\text{mm}$ , there is a higher concentration of oil at the core ( $\alpha_o = 0.217$ ) as compared with the annulus ( $\alpha_o = 0.208$ ). At  $C_L = 0.10$  and  $d = 8.0\text{mm}$ , there is a higher concentration of oil at the core ( $\alpha_o = 0.226$ ) as compared with the annulus ( $\alpha_o = 0.182$ ).

At  $C_L = 0.50$  and  $d = 1.0\text{mm}$  or  $2.0\text{mm}$ , oil appears to be scattered ( $\alpha_o = 0.214$ ). At  $C_L = 0.50$  and  $d = 4.0\text{mm}$ , there is a higher concentration of oil at the core ( $\alpha_o = 0.223$ ) as compared with the annulus ( $\alpha_o = 0.194$ ). At  $C_L = 0.50$  and  $d = 8.0\text{mm}$ , there is a higher concentration of oil at the core ( $\alpha_o = 0.381$ ) as compared with the annulus ( $\alpha_o = 0.182$ ). From the results, we can deduce that when the oil drop diameter increases, there is a higher tendency for oil to coagulate at the core displacing water to the annulus. This displacement effect is more significant when the lift coefficient increases from 0.10 to 0.50 and the oil drop diameter increases from 1.0mm to 8.0mm. However, at  $C_L = 0.10$  or 0.50, the oil core remains at the centre which does not resemble closely with the experiment.

The plot of pressure drop reduction factor versus oil drop diameter at  $J_o = 0.64\text{m/s}$  and  $J_w = 2.20\text{m/s}$  is shown in Figure 4. The pressure drop reduction factor,  $R$  as given in the work by Sotgia *et al.* (2008) is defined as  $R = \Delta P_o / \Delta P_{ow}$ , where  $\Delta P_{ow}$  is the calculated pressure drop of the two-fluid flow and  $\Delta P_o$  is the pressure drop calculated using the Hagen-Poiseuille law for the single-phase laminar flow of oil having the same flow rate as the oil phase in the two-phase flow. The Hagen-Poiseuille law is given by the following equation:  $\Delta P = (128 \mu L Q) / (\pi D^4)$ , where  $\Delta P$  is the pressure drop,  $L$  is the length of pipe,  $\mu$  is the dynamic viscosity,  $Q$  is the volume flow rate and  $D$  is the pipe diameter.

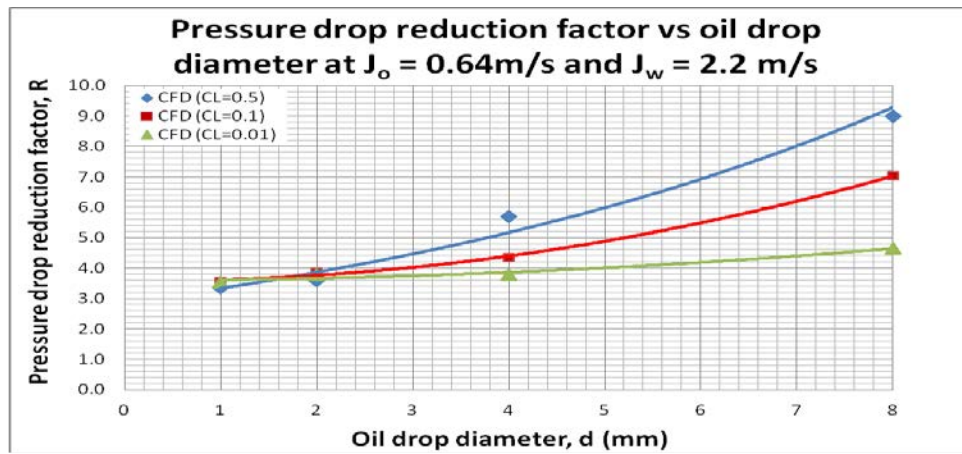


**Figure 4. Plot of pressure drop reduction factor versus oil drop diameter at  $J_o = 0.64\text{m/s}$  and  $J_w = 2.20\text{m/s}$  for dispersed flow. For all  $C_L$ , when oil drop diameter,  $d$  increases from 4.0mm to 8.0 mm, pressure drop reduction factor,  $R$  also increases. The increase in  $R$  is more significant for higher  $C_L$ .**

In general, when the oil drop diameter is between 1.0mm to 2.0mm, the lift coefficient,  $C_L$  does not appear to have a significant effect on the pressure drop reduction factor. When the oil drop diameter is between 2.0mm and 8.0mm and the lift coefficient is increased from 0.01 to 0.50, the pressure drop reduction factor increases. This is because when the lift coefficient increases, there is a higher tendency for the oil droplets to coagulate at the core which is lubricated by a higher concentration of water at the annulus. This reduces the pressure gradient, causing the pressure drop reduction factor to increase. However, it should be noted that a lift coefficient of 0.50 is only for inviscid flow. It is suggested that the lift coefficient to be between 0.01 and 0.10 (Madhavan, 2005) for low viscosity oil.

In comparison with the oil-water distribution from experiment, the phase contour at  $C_L = 0.01$  and  $d = 4.0\text{mm}$  or  $8.0\text{mm}$  is more consistent with the experiment as compared with the phase contour at  $C_L = 0.10$  or  $0.50$ . At  $C_L = 0.10$  or  $0.50$  and  $d = 4.0\text{mm}$  or  $8.0\text{mm}$ , the oil core is concentric at the core. However, at  $C_L = 0.01$  and  $d = 4.0\text{mm}$  or  $8.0\text{mm}$ , the oil core was displaced vertically upwards from the centre. From the results, we may draw the conclusion that the lift coefficient for viscous oil may be  $0.01$  with an equivalent oil drop diameter between  $4.0\text{mm}$  to  $8.0\text{mm}$ .

### 3.3. Effects of mixture velocity

The effects of mixture velocity on pressure drop reduction factor were investigated at  $J_o = 0.64 \text{ m/s}$  and  $J_w = 2.20\text{m/s}, 2.30\text{m/s}, 2.40\text{m/s}, 2.50\text{m/s}$  and  $2.60\text{m/s}$ . The plot of volume fraction of oil at different mixture velocities for  $C_L = 0.01$  and oil drop diameter  $d = 4.0\text{mm}$  and  $8.0\text{mm}$  is shown in Figure 5. For  $d = 4.0\text{mm}$ , when water superficial velocity increases from  $2.2\text{m/s}$  to  $2.6\text{m/s}$ , the volume fraction of oil at the core decreases from  $0.226$  to  $0.213$  respectively. The volume fraction of oil at the annulus decreases from  $0.213$  to  $0.156$  respectively. For  $d = 8.0\text{mm}$ , when the water superficial velocity increases from  $2.2\text{m/s}$  to  $2.6\text{m/s}$ , the volume fraction of oil at the core decreases from  $0.238$  to  $0.213$  respectively. The volume fraction of oil at the annulus decreases from  $0.197$  to  $0.156$  respectively. The results show that when the mixture velocity increases, the volume fraction of oil at the core and annulus decreases. This can be attributed to the fact that when the mixture velocity increases, the higher turbulence effect of water causes the oil droplets to become more dispersed.

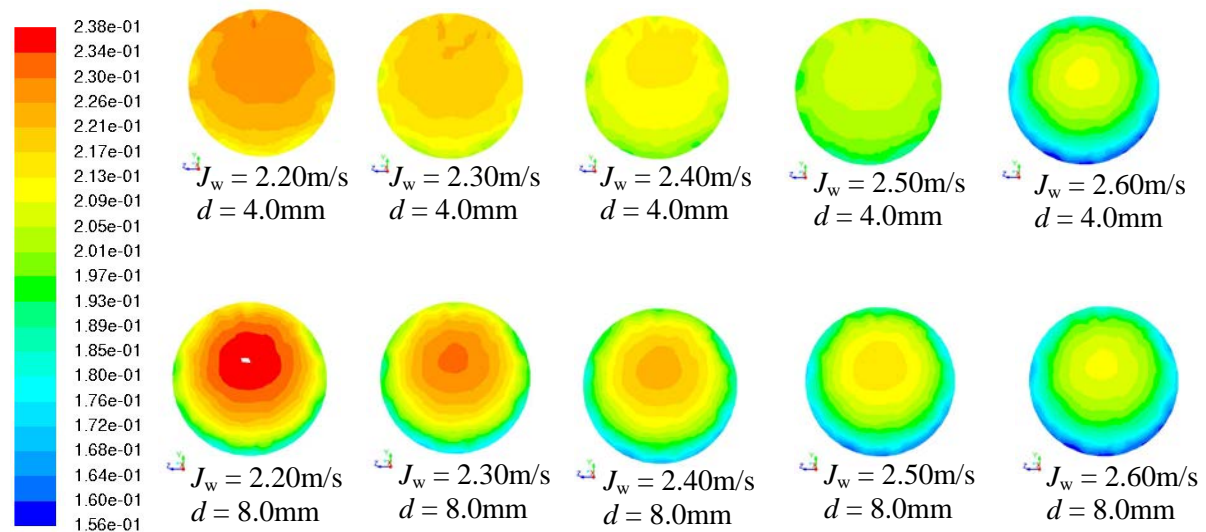


**Figure 5. Plots of oil volume fraction for different water superficial velocities  $J_w$ . Oil drop diameters  $d = 4.0\text{mm}$  and  $8.0\text{mm}$ . Constant parameters are lift coefficient  $C_L = 0.01$  and oil superficial velocity  $J_o = 0.64\text{m/s}$ . When  $J_w$  increases from  $2.20\text{m/s}$  to  $2.60\text{m/s}$ , oil concentration decreases. There is a tendency the oil droplets to congregate at the centre of the pipe forming a core-annular-like flow.**

In addition, when the oil drop diameter increases from  $4.0\text{mm}$  to  $8.0\text{mm}$ , the volume fraction of oil at the core increases but that at the annulus remains constant. This can be attributed to the fact that when the oil drop diameter increases, there is a higher tendency for the oil droplets to concentrate at the core. For all flow regimes, the oil core is displaced vertically upwards from the centre which is consistent with the flow pattern in experiments. CFD

simulations also show that when the water superficial velocity,  $J_w$ , increases, the pressure drop reduction factor,  $R$ , increases marginally. In addition, when the oil drop diameter,  $d$ , increases from 4.0mm to 8.0mm, the pressure drop reduction factor,  $R$ , also increases. It appears that it is more desirable to increase the water superficial velocity as this helps to increase the pressure drop reduction factor. In addition, it is also more desirable to have a larger oil drop diameter as this helps to promote coagulation of the oil droplets at the core, which helps to increase the pressure drop reduction factor (i.e. reduce the pressure gradient). These are interesting observations which has not been reported before in other works. This knowledge is of practical importance for oil industry as it helps to reduce the overall energy required to transport viscous oil along horizontal pipes.

### 3.4. Effects of water input ratio, $\epsilon_w$

Figure 6 shows the plot of pressure drop reduction factor,  $R$ , versus water input ratio,  $\epsilon_w$ , for dispersed flow with  $d = 4.0\text{mm}$  and  $8.0\text{mm}$ . The lift coefficient  $C_L$  is kept constant at 0.01. The oil superficial velocity is kept constant at  $0.64\text{m/s}$  and water superficial velocity is between  $2.2\text{m/s}$  to  $2.6\text{m/s}$ . The simulation results show that when the water input ratio,  $\epsilon_w$  increases from 0.775 to 0.800, there is a marginal increase in the pressure drop reduction factor,  $R$ . This is consistent with the flow physics as when the water input ratio increases, the superficial velocity of water also increases which increases the turbulent intensity of the mixture. The higher turbulence effect of water causes greater dispersion of oil in water. Hence, the pressure gradient decreases and pressure drop reduction factor,  $R$  increases.

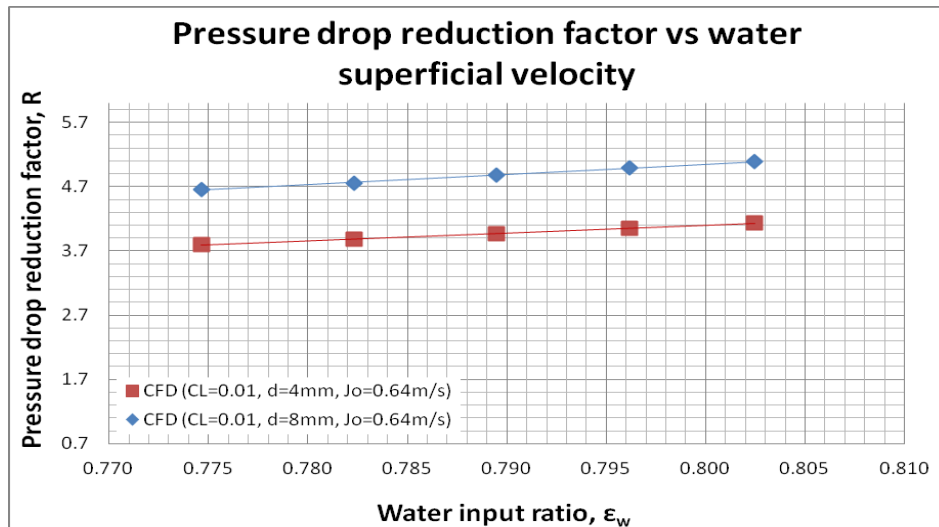


**Figure 6. Plot of pressure drop reduction factor versus water input ratio for dispersed flow. Oil superficial velocity,  $J_o$ , is kept constant at  $0.64\text{m/s}$  and water superficial velocity,  $J_w$ , varies from  $2.2\text{m/s}$  to  $2.6\text{m/s}$ .**

## 4. Conclusions

Dispersed flow of viscous oil and water in a horizontal pipe of  $5.0\text{m}$  long and  $26.0\text{mm}$  in diameter were simulated using the Eulerian-Eulerian multiphase model. The water is treated as the continuous phase and the oil is treated as the dispersed phase modeled as spheres with finite diameters. For the low volume fraction of oil in the system ( $\sim 0.225$ ), the mixture is assumed to be of Newtonian fluid. The simulations suggest that positive lift coefficient,  $C_L$ ,

on the oil droplet is more consistent with experimental observation. In particular, when  $C_L = 0.01$  and oil drop diameter,  $d = 4.0\text{mm}$  or  $8.0\text{mm}$ , the phase contour of the dispersed phase at the core is displaced vertically upwards which is more consistent with experiment. The CFD simulation results also show that it is desirable to have a larger oil drop diameter as this helps to increase the pressure drop reduction factor. When the oil superficial velocity,  $J_o$ , remains constant at  $0.64\text{m/s}$  and water superficial velocity,  $J_w$ , increases from  $2.20\text{m/s}$  to  $2.60\text{m/s}$ , the volume fraction of oil for the dispersed phase decreases due to the higher turbulence effect of water. In addition, it appears that it is more desirable to have a higher water superficial velocity as this helps to increase the pressure drop reduction factor,  $R$  marginally. This reduces the overall pressure gradient which helps to improve the efficiency of transportation of viscous oil.

### References

1. Alboudwarej, H, Felix, J, Taylor, S, 2006. Highlighting Heavy Oil. Oilfield Review.
2. Bannwart, A.C., Rodriguez, O.M.H., Carvalho, C.H.M., Wang, I.S. and Vara, R.M.O., 2004. Flow Patterns in Heavy Crude Oil-Water Flow. Trans. ASME, 126, pp. 184 – 189.
3. Bannwart, A.C., Rodriguez, O.M.H. and Biazussi, J.L., 2012. Water-assisted Flow of Heavy Oil in a Vertical Pipe: Pilot-scale Experiments. Int. J. Chem. Reactor Eng., 10, pp. 1 – 16.
4. Hu, B. and Angeli, P, 2006. Phase inversion and associated phenomena in oil-water vertical pipeline flow. The Canadian J. Chem. Eng., 84, pp. 1 – 14.
5. Sogtia, G., Tartarini, P. and Stalio, E., 2008. Experimental analysis of flow regimes and pressure drop reduction in oil-water mixtures. Int. J. Multiphase Flow 34, pp. 1161 – 1174.
6. Lovick, J. and Angeli, P., 2004. Experimental studies on the dual continuous flow pattern in oil-water flows. Int. J. Multiphase Flow, 30, pp. 139 – 157.
7. Charles, M.E, Govier, G.W. and Hodgson, G.W., 1961. The horizontal pipeline flow of equal density oil-water mixtures. The Canadian J. Chem. Eng., 39, pp. 27 – 36.
8. Bai, R.Y., Chen, K.P and Joseph, D.D., 1992. Lubricated pipelining: Stability of core-annular flow. Part 5. Experiments and comparison with theory. J. Fluid Mech., 240, pp. 97 – 132.
9. Madhavan, S., 2005. CFD Simulation of Immiscible Liquid Dispersions. MSc Thesis, Dalhousie University, Canada.
10. Wang, W., Gong, J. and Angeli, P., 2011. Investigation on heavy crude-water two phase flow and related flow characteristics. Int. J. Multiphase Flow, 37, pp. 1156 – 1164.